

RECENT SEISMIC ACTIVITY ALONG THE HELLENIC VOLCANIC ARC

G. STAVRAKAKIS, G. CHOULIARAS and M. SACHPAZI

National Observatory of Athens, Institute of Geodynamics,
P.O. Box 20048, 11810 Athens, Greece.

SUMMARY

Twenty nine well recorded earthquakes from the volcanic islands of Nisyros and Santorini during 1995-1996 have been chosen for spectral analysis in order to determine their seismic source parameters. The results indicate that the Nisyros data set and the Santorini events until the end of 1995 follow scaling relations similar to those of other seismic regions. However most of the 1996 data set for Santorini and in particular the May 27 1996 seismic sequence, exhibit unique seismic source characteristics when compared to the rest of the data set. This result may be associated with very recent geodetic results showing that a caldera inflation episode occurred on the island reaching a maximum in March 1996.

INTRODUCTION

One of the main geophysical properties of the Hellenic arc is a well defined Benioff zone due to the underthrusting of the African lithosphere beneath the Aegean¹. This Benioff zone is dipping at about 40° from the convex to the concave part of the arc and the maximum depth is around 190 km. The Volcanic arc of the south Aegean (figure 1) associated with this subduction is comprised of three Quarternary volcanoes namely Santorini, Nisyros and Methana and solfatara and fumarole fields in Sousaki and Milos².

Along this volcanic arc a seismogenetic layer at a depth of 20 km overlies an aseismic layer down to a depth of 120 km. Below this aseismic layer lies another seismic layer to a depth of 180 km. The distribution of intermediate earthquakes in this layer define the top surface of the Benioff zone³. Epicentres of strong shallow and intermediate earthquakes have been grouped into five well defined clusters each corresponding to the five volcanic centres mentioned above⁴.

In August 1995 an increase in the seismic energy release was observed in the volcanic islands of Santorini and Nisyros. The largest of these events occurred in April 1996 when a $M_L=5.0$ intermediate depth earthquake took place in Nisyros while in May 1996 a shallow depth seismic sequence with a $M_L=4.2$ main shock took place in Santorini.

Digital seismological data for the period 1995-1996, concerning seismic events in Nisyros and Santorini, have been recorded by two short period digital networks operated by the Institute of Geodynamics of the National Observatory of Athens. One is the "Lenet" network configured with eight Lennartz MARS88/MC stations in different locations around Greece and the other is the "Sanet" network configured with eight Teledyne stations in Santorini and the surrounding region (figure 2). Both networks are operated on trigger mode using the classic LTA/STA criterion and

communication of the remote stations with the host computer in Athens is achieved via dial-up public telephone lines. It is the purpose of this study to perform spectral analysis on the P and S wave data from 29 well recorded seismic events during 1995-1996 from Nisyros and Santorini in order to determine their source parameters and to further examine the seismic moment versus magnitude and seismic moment versus source size relations.

METHODOLOGY

Source parameter determination from spectral analysis of P or S wave data has been the focus of many studies and good examples include the pioneer works of Keilis-Borok⁵, Hanks and Wyss⁶, Thacher and Hanks⁷.

The analysis procedure used in this study employs the PITSA signal processing toolbox⁸ and it involves Fourier spectral analysis of selected time windows in the displacement trace which is always corrected for the appropriate instrument response. A Fourier analysis is performed on a time window that contains noise and in addition to this a Fourier spectral analysis is performed on a window of same duration containing, in the case of a vertical component seismometer, a P-wave and in the case of a horizontal component seismometer, the S-wave of the transverse component. The noise spectra are then used to correct the P and S wave spectra and after this interactive spectral fitting is performed using a Brune source model^{9,10} and the nonlinear Marquardt-Levenberg inversion¹¹ to recover the spectral parameters using a constant value for the whole path absorption factor Q. This inversion problem is described in detail by Scherbaum¹².

The characteristics of the source for a seismic event are determined from the two parameters of the P or S wave log-displacement spectra. These parameters are the long period spectral level Ω_0 , and the spectral corner frequency f_c .

A general feature of all dislocation models is that the long period level Ω_0 is proportional to the seismic moment and that the corner frequency f_c is inversely proportional to the source dimension, r .

Following Keilis-Borok⁵ :

$$M_0_{(p,s)} = \frac{(4\pi \cdot \rho \cdot v_{(p,s)}^3 \cdot \Omega_{0(p,s)} \cdot R)}{(k \cdot R\theta\varphi_{(p,s)})} \quad (1)$$

where $\rho = 2.64 \text{ g/cm}^3$ is the density of the medium, R is the hypocentral distance between the source and the receiver, $v_{p,s}$ are the P or S wave velocities near the source with $v_p = 6 \text{ km/sec}$ and $v_s = 3.3 \text{ km/sec}$, k is the free surface operator = 2 and $R_{(p,s)} = 0.5$ is the average radiation pattern coefficient. Logarithmic weighted averages over all records have been computed¹³ to obtain mean long period spectral levels and seismic moments.

Source radii have been computed using the corner frequencies $f_{c(p,s)}$ also by weighted logarithmic averages based on the models of Brune^{9,10} and Madariaga¹⁴ :

$$\text{Brune model} \quad r = \frac{0.37 V_{(p,s)}}{f_{C(p,s)}} \quad (2)$$

$$\text{Madariaga model} \quad r = \frac{0.32 V_s}{f_{C(p)}} = \frac{0.21 V_s}{f_{C(s)}} \quad (3)$$

Stress drops ($\Delta\sigma$) and average displacement on the fault plane ($\langle u \rangle$) have been computed from the mean values of moments and source radii of P and S waves accordingly^{5,15} :

$$\Delta\sigma = \frac{0.44 M_0}{r^3} \quad (4)$$

$$\langle u \rangle = \frac{M_0}{\pi \mu r^2} \quad (5)$$

where $\mu = 3 \times 10^{11}$ dyne/cm is the rigidity of the medium.

RESULTS AND DISCUSSION

Table 1 lists the seismic events considered in this study together with their epicentral coordinates and magnitudes as determined from the monthly bulletins of the National Observatory of Athens.

The Nisyros data include four intermediate and twelve shallow earthquakes with $M_L=3.6-5.0$ while the Santorini data set has one intermediate event and twelve shallow events with $M_L=3.3-4.2$. In Figure 2 we note that most of the Nisyros events are distributed along a E-W direction between Kos and Nisyros (figure 3) while the Santorini events cluster to the NE of the island (figure 4). Figure 5 shows a sample recording of a $M_L=5.0$ event from Nisyros from the Lenet network showing very good signal to noise ratio and good detectability even by distant stations. Figure 6 shows the P wave displacement trace of a $M_L=4.2$ event from Santorini as recorded by a Sanet station on the island and the resulting displacement spectrum indicating a constant background level and a clear corner frequency.

Table 2 lists the seismic moments, corner frequencies, source radii, average displacements and stress drops for the events under study, for two different source models namely Brune's and Madariaga's. As expected from seismic source theory Madariaga's model results in smaller source dimensions and larger average displacements and stress drops in comparison to the results from Brune's source model.

Figure 7 shows the moment versus magnitude relation and the moment versus corner frequency relation for our two data sets. The Nisyros data show a tendency for a linear moment-magnitude relation similar to other seismic regions from Greece¹⁶ but the Santorini data show great deviations.

In the moment-corner frequency data also on figure 7 the Nisyros and some of the Santorini data show a tendency for a decrease in

seismic moment with corner frequency which is also in agreement with other seismic regions in Greece but a group of seven events from the Santorini data set (54%) have a constant corner frequency around 2.5 Hz irrespective of seismic moment. Such a behaviour can be due to fresh ruptures that nucleate in regions of high stress and stop gradually when encountering low stress zones¹⁷. This type of physical model could be justified in a volcanic area by the presence of a heterogeneous stress distribution in the seismogenic volume. A similar result has been observed for the microearthquakes in the Phlegraean Fields volcanic area in Southern Italy¹⁸.

For Santorini in particular, all the events from the May 27 1996 seismic sequence and one event from February 18 1996 have a constant source radius irrespective of the seismic energy they release, unlike tectonic earthquakes. This anomalous behaviour in the seismic source dimension for these earthquakes may be related to volcanic processes since continuous geodetic measurements on Santorini since 1994 show that a minor and slow episode of caldera inflation by about 4-6 cm occurred in the beginning of 1996 and reached a maximum in March 1996¹⁹. In the light of these recent results a more thorough multidisciplinary investigation is required in order to interpret the observations regarding the volcano of Santorini.

REFERENCES

- (1) Papazachos B.C. and Comninakis, P.E., 1969. Geophysical features of the greek island arc and Eastern Mediterranean ridge. Proceedings of the C.R. Conf. Madrid, Publ. J.P. Rothe, 16, 74-75.
- (2) Papazachos B.C. and Comninakis, P.E., 1971. Geophysical and tectonic features of the Aegean arc. J. Geophys. Res., 76, 8517-8533.
- (3) Papadopoulos, G.A., Kondopoulou, D., Leventakis, G. A. and Pavlides, S.B., 1986. Seismotectonics of the Aegean region. Tectonophysics, 124, 67-84.
- (4) Papazachos B.C. and Panagiotopoulos, D.G., 1993. Normal faults associated with volcanic activity and deep rupture zones in the southern aegean volcanic arc. Tectonophysics, 220, 301-308.
- (5) Keilis-Borok., 1959. On the estimation of the displacement in an earthquake source and of source dimensions. Ann.Geof., 12, 205-214.
- (6) Hanks, T.C. and Wyss, M., 1972. The use of body wave spectra in the determination of seismic source parameters. Bull. seism. Soc. Am., 62, 561-589.
- (7) Thatcher, W. and Hanks, T.C., 1973. Source parameters of southern California earthquakes. J. Geophys. Res., 78, 8547-8576.
- (8) Sherbaum, F., and Johnston, J., 1993. PITSA, IASPEI Software library, Vol. 5, 1993.
- (9) Brune, J.N., 1970. Tectonic stress and the spectra of seismic shear waves from earthquakes. J. Geophys. Res., 75, 4997-5009.
- (10) Brune, J.N., 1971. Correction. J. Geophys. Res., 76, 5002.

- (11) Marquardt, D.W., 1963. An algorithm for least squares estimation of nonlinear parameters. *J. Soc. Ind. Appl. Math.*, 11, 431-441.
- (12) Scherbaum, F., 1990. Combined inversion for the three-dimensional Q structure and source parameters using microearthquake spectra. *J. Geophys. Res.*, 95, 12423-12438.
- (13) Archuleta, R.J., Granswick, E., Mueller, C, and Spudich, P., 1982. Source parameters of the 1980 Mammoth Lakes, California, earthquake sequence. *J. Geophys. Res.*, 87, 4595-4607
- (14) Madariaga, R., 1976. Dynamics of an expanding circular fault. *Bull. seism. Soc. Am.*, 66, 636-666.
- (15) Brune, J.N., 1968. Seismic moment, seismicity and rate of slip along major fault zones. *J. Geophys. Res.*, 73, 777-794.
- (16) Chouliaras, G. and Stavrakakis, G. 1996. Seismic source parameters from a dial-up seismological network in Greece. *Pageoph.* (in print).
- (17) Hussein, M.I, Jovanovich, B.B., Randal, M.J. and Freund, J.B. The fracture energy of earthquakes. *Geophys. J.*, 43, 367-385.
- (18) Del Pezzo, E, De Natale, G., Martini, M., and Zollo A., 1987. Source parameters of microearthquakes at Phlegraean Fields volcanic area. *Physics of the Earth and Planetary Interiors*, 47, 25-42.
- (19) Stiros, S.C., 1996. Geodetic control of small topographic changes, Santorini volcano. Final report to the E.E.C. DG XII, Environment, Natural Hazards, Contract EV5V-CT93-0285.

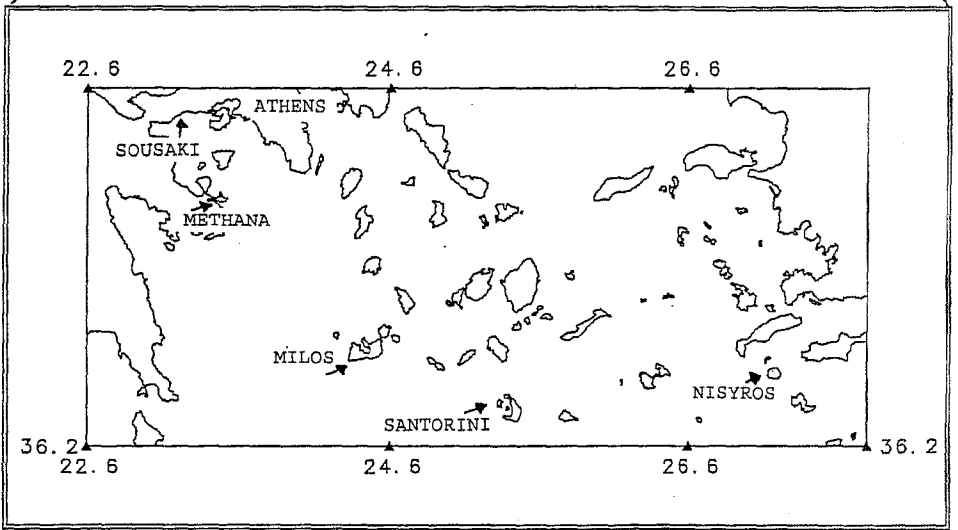
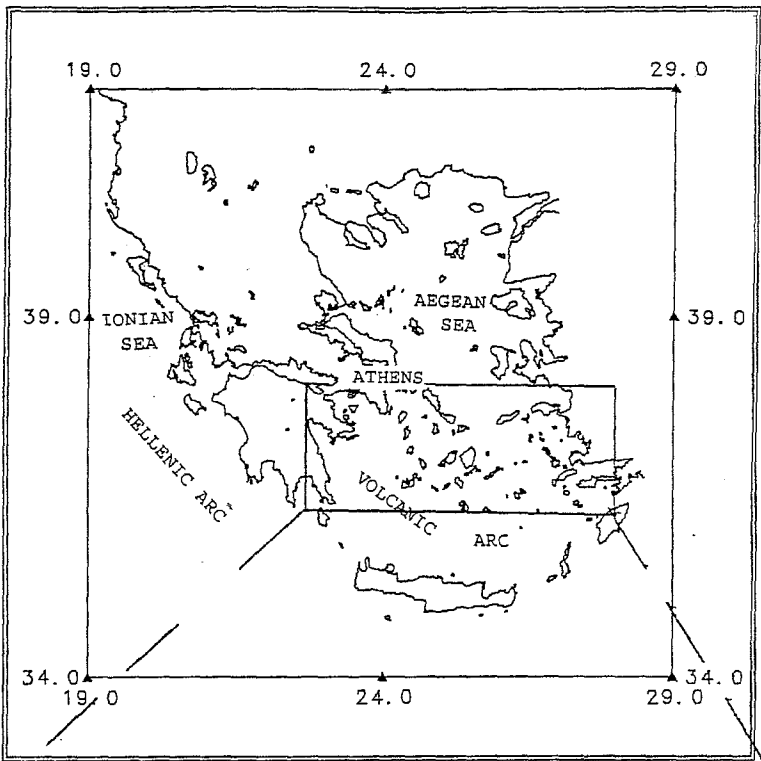


Figure 1 : Map of Greece (upper) and map of the volcanoes in the Hellenic volcanic arc (lower).

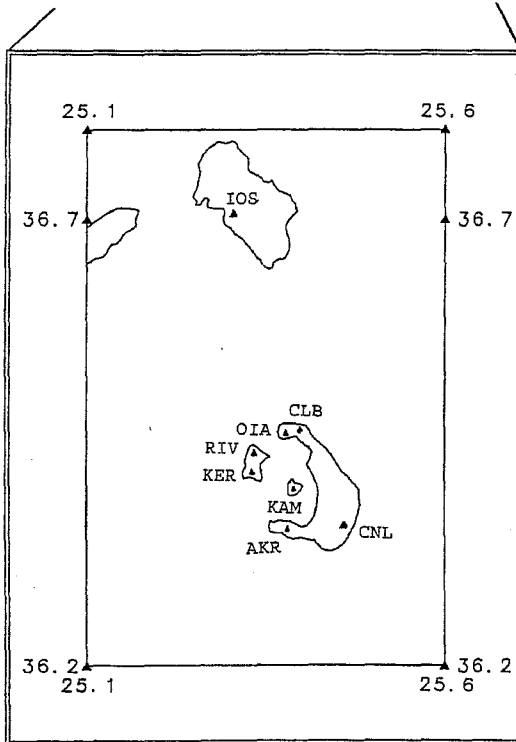
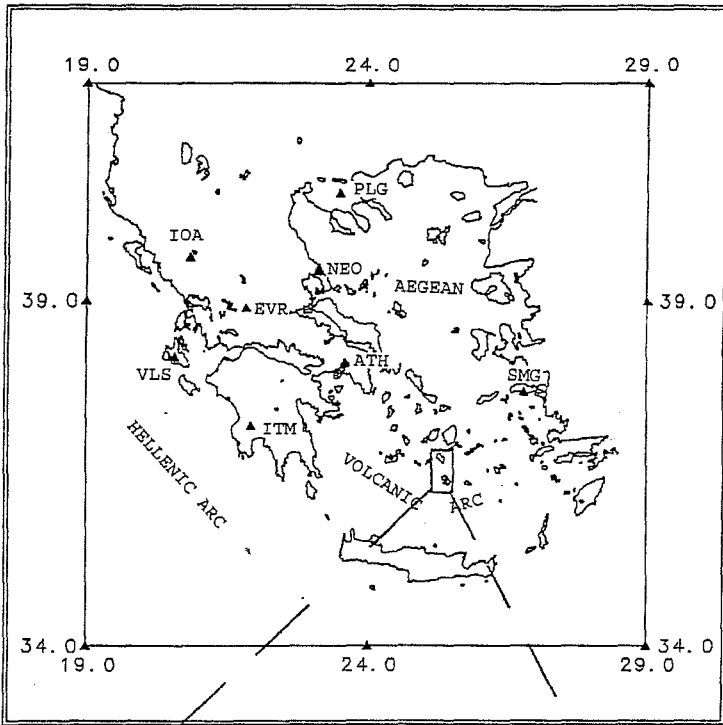


Figure 2 : Map of the Lenet network (upper) and map of the Sanet network in Santorini (lower).

Table 1: Catalog of earthquakes used in this study

No	Date	Time (GMT)	Lat N	Lon E	Z (km)	M
NISYROS						
1	1995 AUG 22	05 34 18.8	36.62	26.73	165	4.9
2	1995 SEP 11	08 12 59.3	36.60	26.91	32	3.8
3	1995 SEP 21	23 52 44.2	36.56	26.71	38	4.3
4	1995 NOV 25	09 16 39.9	36.61	27.25	37	3.6
5	1995 NOV 27	13 26 5.2	36.44	27.33	39	4.0
6	1995 NOV 30	11 49 35.6	36.59	27.12	130	4.8
7	1995 DEC 14	20 53 24.5	36.50	27.38	5	3.9
8	1995 DEC 18	07 49 8.4	36.54	26.98	38	3.5
9	1996 JAN 2	15 14 36.3	36.56	27.04	10	3.6
10	1996 JAN 2	20 51 23.8	36.64	27.25	37	3.7
11	1996 FEB 18	20 03 6.5	36.69	27.22	5	3.7
12	1996 FEB 21	07 04 13.8	36.32	27.10	3	3.9
13	1996 APR 12	15 39 11.6	36.62	27.09	156	5.0
14	1996 APR 27	21 41 51.8	36.68	27.27	10	3.8
15	1996 MAY 15	06 02 24.4	36.61	27.17	10	3.8
16	1996 MAY 21	14 52 20.6	36.58	26.71	149	4.2

SANTORINI

1	1995 AUG 16	02 30 11.6	36.45	25.45	33	3.4
2	1995 OCT 29	05 37 49.4	36.56	25.49	27	3.3
3	1995 NOV 23	17 06 24.6	36.60	25.69	5	3.6
4	1995 NOV 23	17 10 12.4	36.69	25.64	9	3.7
5	1996 FEB 18	21 30 52.1	36.55	25.55	29	3.6
6	1996 MAR 30	00 03 52.0	36.54	25.56	16	3.6
7	1996 MAY 10	07 55 32.3	36.52	25.32	120	3.5
8	1996 MAY 27	12 36 .7	36.54	25.51	17	3.8
9	1996 MAY 27	14 25 35.0	36.52	25.47	8	4.1
10	1996 MAY 27	14 35 48.1	36.46	25.50	5	3.5
11	1996 MAY 27	14 56 47.6	36.52	25.48	10	4.2
12	1996 MAY 27	16 51 53.6	36.53	25.50	18	3.9
13	1996 MAY 27	19 16 38.3	36.57	25.71	5	3.7

Figure 3 : Epicentres of the earthquakes analysed in this study from Nisyros.

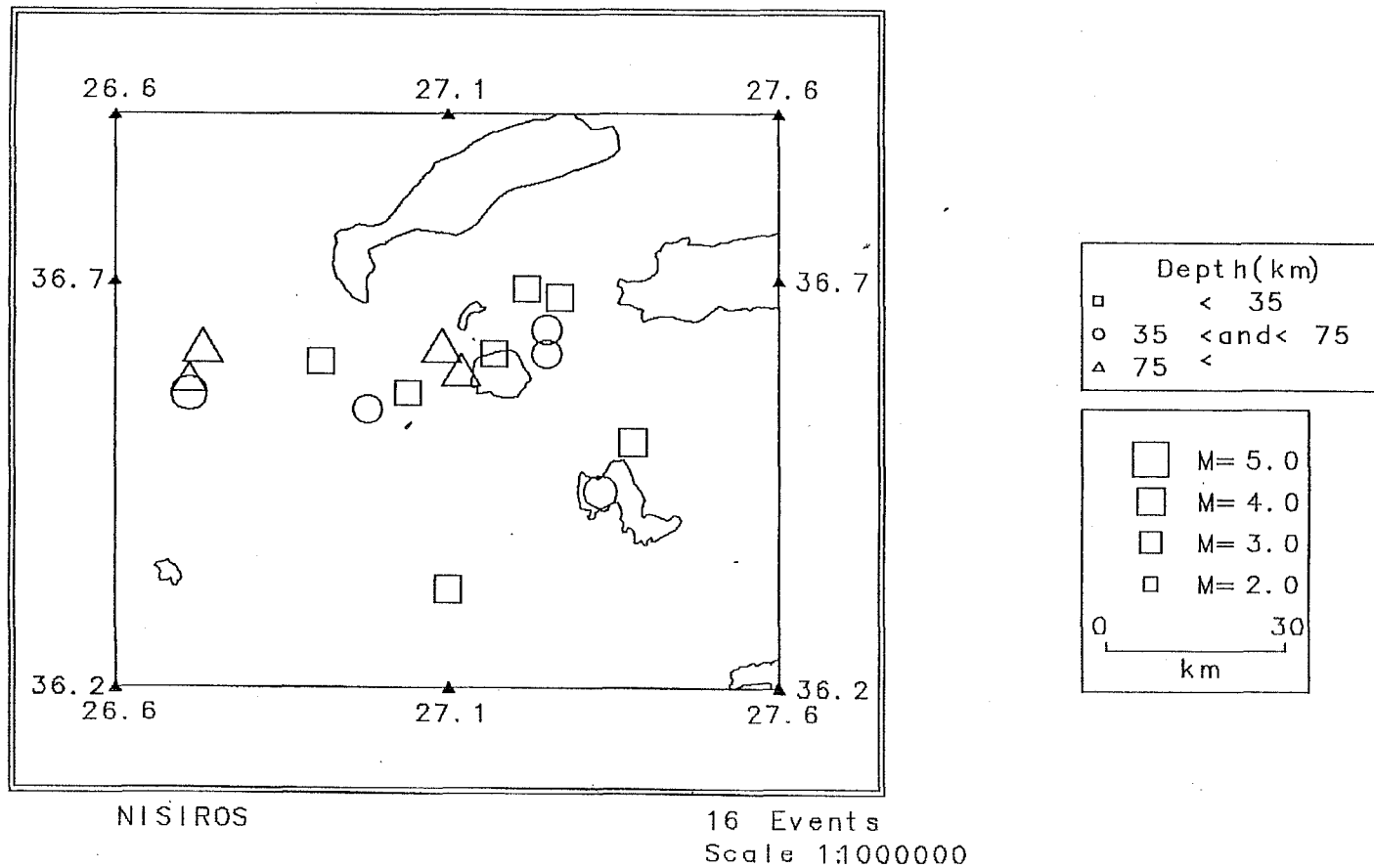
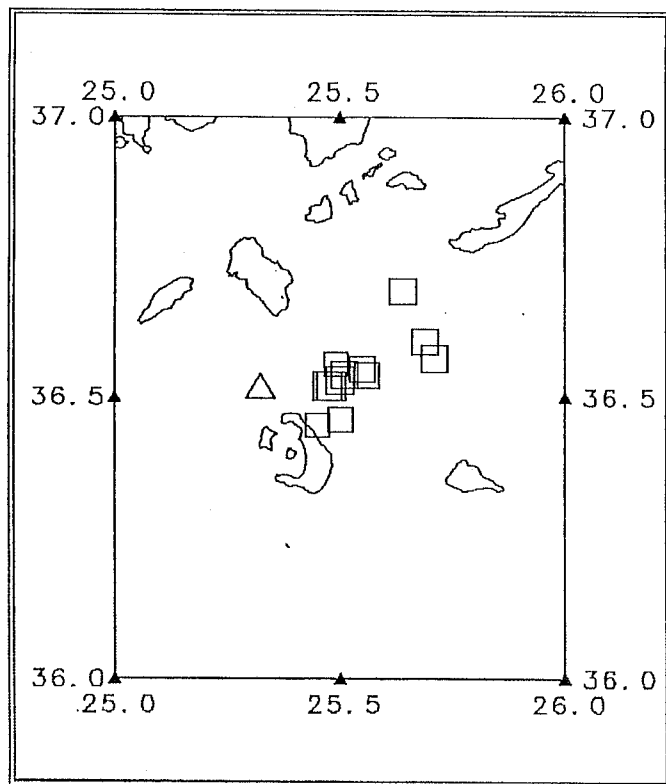


Figure 4 : Epicentres of the earthquakes analysed in this study from Santorini.



Depth (km)

- < 35
- 35 < and < 75
- △ 75 <

- M= 5.0
- M= 4.0
- M= 3.0
- M= 2.0

0 40
km

SANTORINI

13 Events

Scale 1:1500000

Table 2: Seismic source parameters from spectral analysis. M_0 is seismic moment, F_c is the corner frequency, R is the fault radius, D_s is the stress drop and U is the average displacement. Subscripts B and M correspond to Brune and Madariaga models.

No	M_l	M_0 (dyne.cm) (dyne.cm)	F_c (Hz)	R_b (km)	R_m (km)	D_{sb} (bar)	D_{sm} (bar)	U_b (cm)	U_m (cm)
Nisiroi									
1	4.9	5.2930e+024	0.7	3.17	1.51	73.01	678.35	55.84	246.77
2	3.8	1.0292e+023	1.1	2.02	0.96	5.51	51.18	2.68	11.85
3	4.3	1.5173e+024	0.9	2.47	1.17	44.48	413.30	26.46	116.94
4	3.6	5.9987e+022	1.2	1.85	0.88	4.17	38.73	1.86	8.22
5	4.0	3.0876e+022	1.0	2.22	1.06	1.24	11.54	0.66	2.94
6	4.8	1.7996e+024	0.8	2.78	1.32	37.05	344.28	24.80	109.60
7	3.9	5.1459e+022	1.0	2.22	1.06	2.07	19.22	1.11	4.90
8	3.5	2.0584e+022	1.3	1.70	0.81	1.82	16.90	0.75	3.31
9	3.6	3.0876e+022	1.2	1.85	0.88	2.15	19.94	0.96	4.23
10	3.7	3.0876e+022	1.2	1.85	0.88	2.15	19.94	0.96	4.23
11	3.7	2.0584e+022	1.2	1.85	0.88	1.43	13.29	0.64	2.82
12	3.9	8.2335e+022	1.0	2.22	1.06	3.31	30.76	1.77	7.83
13	5.0	1.9996e+024	0.5	4.44	2.11	10.05	93.39	10.76	47.56
14	3.8	2.0584e+023	1.2	1.85	0.88	14.30	132.90	6.38	28.20
15	3.8	2.0584e+023	1.0	2.22	1.06	8.23	76.91	4.43	19.59
16	4.2	2.0584e+023	0.8	2.78	1.32	4.24	39.38	2.84	12.53
Santorini									
1	3.4	2.7053e+023	0.9	2.47	1.17	7.93	73.69	4.72	20.85
2	3.3	5.1459e+022	1.1	2.02	0.96	2.76	25.59	1.34	5.92
3	3.6	3.0876e+022	1.2	1.85	0.88	2.15	19.93	0.96	4.23
4	3.7	1.3526e+023	1.0	2.22	1.06	5.43	50.54	0.91	12.87
5	3.6	3.0876e+022	2.5	0.89	0.42	19.40	180.26	4.15	18.36
6	3.6	3.0876e+022	0.9	2.47	1.17	0.90	8.41	0.54	2.38
7	3.5	1.0292e+023	0.8	2.78	1.32	2.12	19.69	1.42	6.27
8	3.8	2.0584e+023	2.5	0.88	0.42	129.34	1201.70	27.70	122.41
9	4.1	2.1466e+022	2.5	0.88	0.42	13.48	125.32	2.89	12.77
10	3.5	1.0821e+022	2.5	0.88	0.42	6.80	63.18	1.46	6.43
11	4.2	6.7632e+021	2.5	0.88	0.42	4.24	39.48	0.91	4.02
12	3.9	7.2043e+021	2.5	0.88	0.42	4.52	42.06	0.97	4.28
13	3.7	2.7053e+021	2.5	0.88	0.42	1.69	15.79	0.36	1.60

Figure 5 : Digital recording by the Lenet network from a $M_L=5.0$ event from Nisyros.

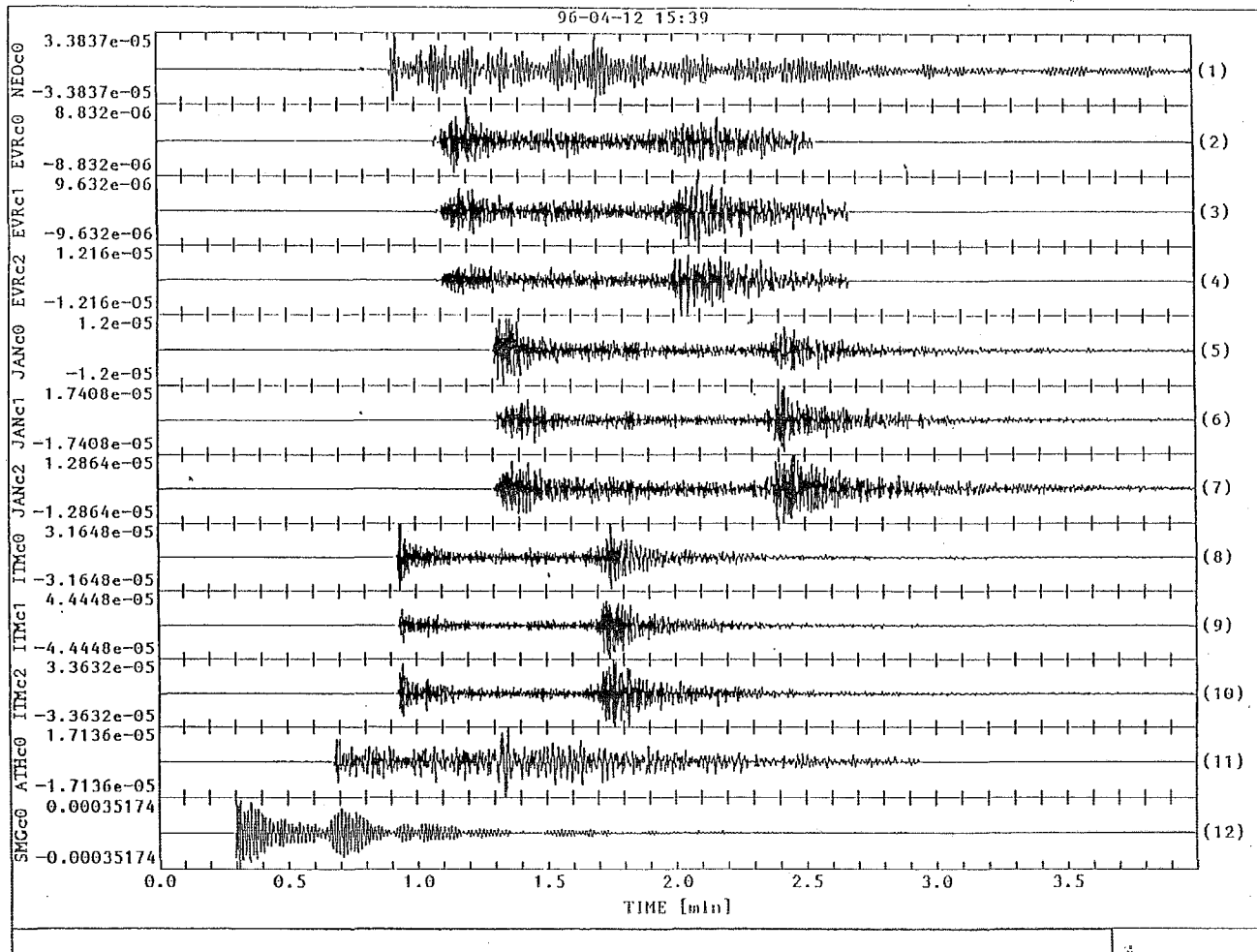
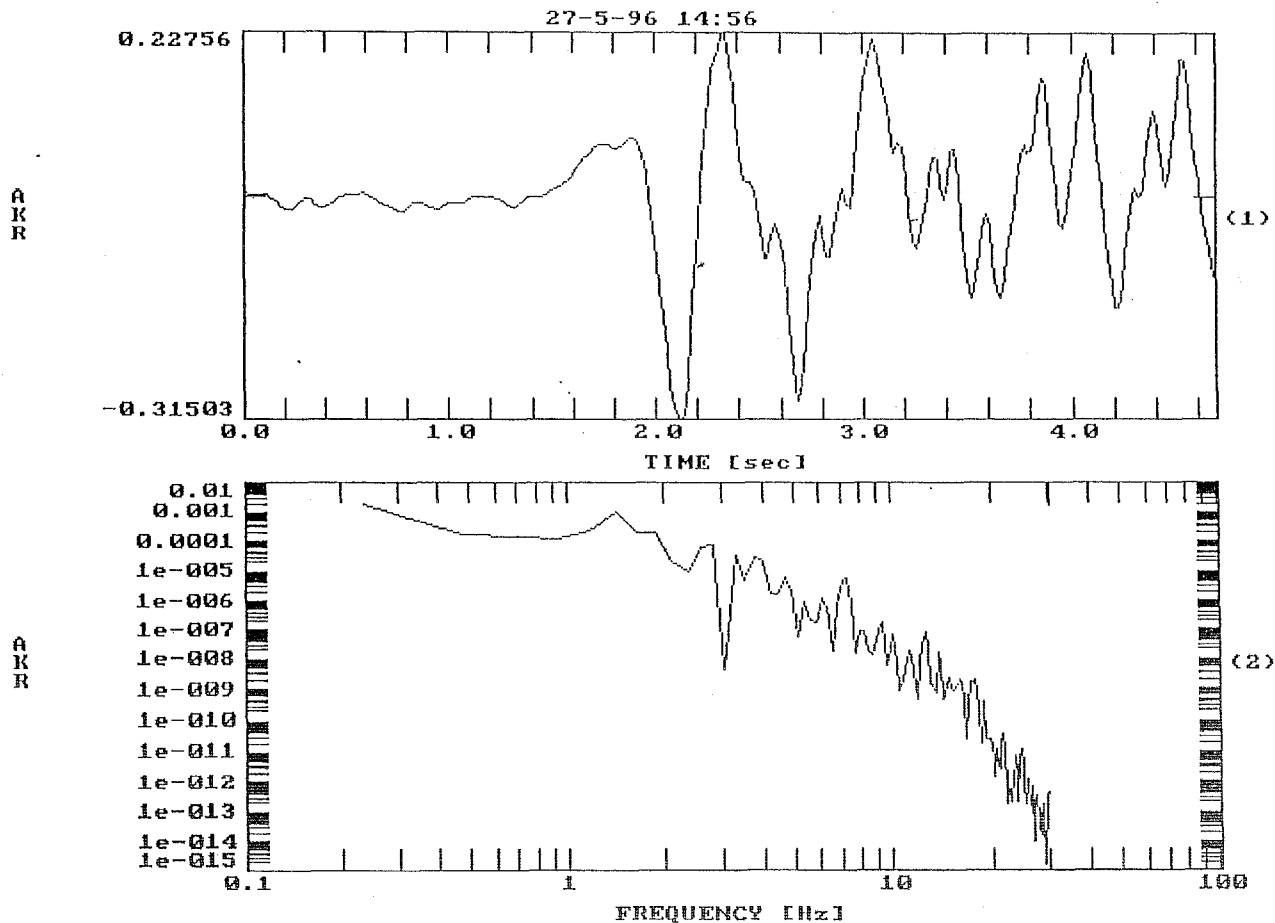


Figure 6 : P-wave displacement trace (1) from the Sanet station AKR in Santorini for a $M_L=4.2$ event in Santorini and the resulting P-wave displacement spectrum (2).



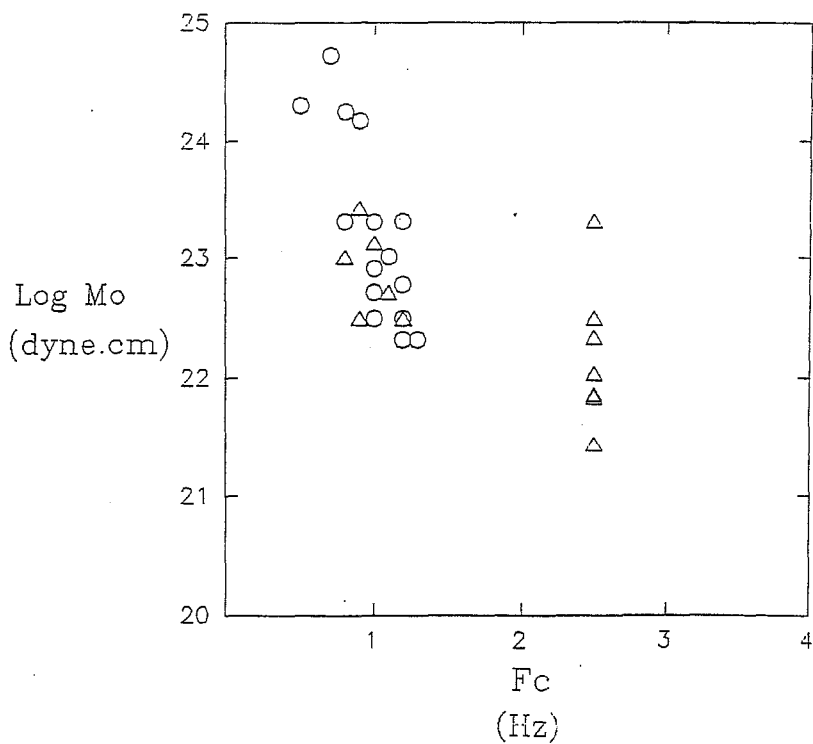
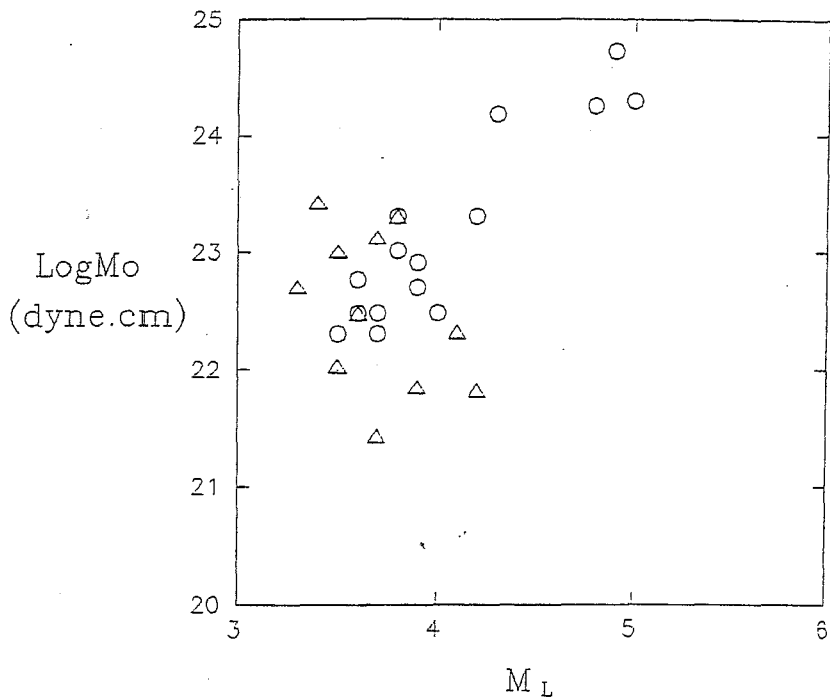


Figure 7 : Log seismic moment versus local magnitude (upper) and Log seismic moment versus corner frequency (lower) for Nisyros earthquakes (circles) and Santorini earthquakes (triangles).